IEEE Access
Multidisciplinary ⋮ Rapid Review ⋮ Open Access Journal

Received 16 January 2023, accepted 14 February 2023, date of publication 16 February 2023, date of current version 13 March 2023.

Digital Object Identifier 10.1109/ACCESS.2023.3246054

RESEARCH ARTICLE

A Multi-Polarization Series-Fed Antenna Array Based on Eccentric Ring

XIN GUAN, ZHENGHUI XUE, WU REN, AND WEIMING LI
School of Integrated Circuits and Electronics, Beijing Institute of Technology, Beijing 100081, China

Corresponding author: Wu Ren (renwu@bit.edu.cn)

This work was supported in part by the National Natural Science Foundation of China under Grant 62071040; and in part by the Beijing Key Laboratory of Millimeter-Wave and Terahertz Wave Technology, School of Integrated Circuits and Electronics, Beijing Institute of Technology.

ABSTRACT A multi-polarization series-fed antenna working at 10 GHz is presented in this paper. The patch elements are built by eccentric rings which can realize the performance of circular polarization. The dual-port feeding allows us to switch the polarization of the antenna. The right-hand circular polarization (RHCP), left-hand circular polarization (LHCP), and Linear polarization (LP) polarization can be realized by properly feeding form. The changing of antenna polarization without switch controlling. Owing to the circular array arrangement, the antenna can form a compact structure. The key features of this array are multi-polarization and traveling-wave series-fed performance. The axial ratios are lower than 3dB measured. The $|S_{21}|$ is lower than -14 dB in the mentioned bandwidth. Then, a 4×4 MIMO array which has compact structure is designed and simulated. The circular array is processed and measured. The experimental and simulation results are in good agreement.

INDEX TERMS Antenna, multi-polarization, traveling-wave series-fed, eccentric ring, circular array.

I. INTRODUCTION

Recently, multifunctional antennas have been improved the development in wireless communication because of they can realize polarization switchable, provide flexible radiation pattern, and reduced the antenna size. Multi-polarization antennas which will be used in radar of ship and satellite can improved signal reception, realize polarization matching.

The realization of circular polarization (CP) function is the focus of multi-polarization. Recently, CP are highly recommended in many applications [1], [2], [3], [4], [5], [6], [7], [8], [9], [10]. Jindong Zhang proposed a dual-CP array antenna which can be realized on a single layer board [1]. Qiang Liu presented a dual-band directional CP antenna, which can be applied to handheld radio-frequency identification reader applications [2]. Reference [3] presents a broadband dual-CP patch antenna and [4] presented a CP square slot antenna for WLAN applications. A dual-polarization CPW-fed slot antenna is proposed for wide bandwidth and high isolation in 2010 [5]. TM10 mode can generate CP operation [6]. An antenna consisted of two eccentric rings which can realize dual CP is proposed [7]. Reference [8], [9], [10], scholars realized CP by using microstrip patches. In the above articles, most of the feeding method in CP antenna structure are single point feeding. What's more, these antennas cannot realize the conversion between circular polarization and linear polarization. To realize polarization switchable performance, it is better to introduce dual port feeding to generate traveling wave transmission form.

Traveling-wave transmission arrays can broaden frequency bandwidth, provide flexible radiation pattern and realize polarization switchable [11], [12], [13], [14], [15], [16]. A CP traveling-wave microstrip array antenna is presented in [11], [12], and [13]. These antennas are consisted of square microstrip patch. But the antenna has a little higher transmission coefficient [11], [12]. And the bandwidth of the given antenna is relatively narrow [13]. For millimeter-wave applications, a dual-CP series-fed antenna is presented [14]. The scholars proposed two-port traveling wave series-fed array for circular polarization [15]. The antenna polarization

The associate editor coordinating the review of this manuscript and approving it for publication was Shah Nawaz Burokur.

This work is licensed under a Creative Commons Attribution-NonCommercial-NoDerivatives 4.0 License.
For more information, see https://creativecommons.org/licenses/by-nc-nd/4.0/

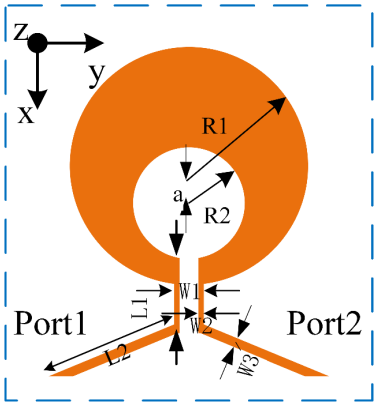

FIGURE 1. Patch unit cell structure. The final design dimensions are: W1 = 1.6 mm, W2 = 0.3 mm, L2 = 7.3 mm, R1 = 6.4mm, R2 = 3.0mm.

will be changed by adjusting the feeding form of the port to realized multi-polarization [16], [17]. Compared with the antenna in the above literature, the antenna proposed in this paper has wider bandwidth, lower isolation and lower transmission coefficient. Meanwhile, the polarization of the antenna can be switched.

In this paper, an eccentric ring unit cell structure which can realize polarization switchable is proposed. By suitable excitation of the ports, the multi-polarization switchable performance can be realized. Then, the unit cell is arranged in circular array. A two-port traveling wave series-fed array is established. The antenna has a simple structure and wide bandwidth. The transmission coefficient is lower than −14 dB in the mentioned frequencies. The axial ratios are lower than 3dB measured. The measured results agree reasonably well with the simulated. This proposed antenna can be used not only in radar and satellites, but also in civilian vehicle speed monitoring. At the same time, the antenna has the function of polarization switching, which can send or receive signals of arbitrary polarization for information matching.

Section II discusses the antenna design current distribution and principle of operation of the unit eccentric ring cell for multi-polarization switchable. In Section III, the two-port traveling wave series-fed circular array is discussed. The simulation results of the 4 × 4 MIMO array antenna are provided. The measured results with the circular array are presented in Section IV. The S-parameter, radiation pattern, axial radio and gain of the proposed antenna are analyzed.

II. UNIT-CELL ANTENNA GEOMETRY

The proposed unit cell is shown in Figure 1, which is consisted of eccentric ring radiated and dual feed. The proposed unit cell structure can achieve multi-polarization with proper port excitation. All simulations are completed in HFSS 2018.

The instantaneous current distributions of the four polarizations are showed in Figure 2(a)–(d). In a time period, the instantaneous current distributions of unit cell will appear a rotation law. In the Figure 2, the black arrow represents the

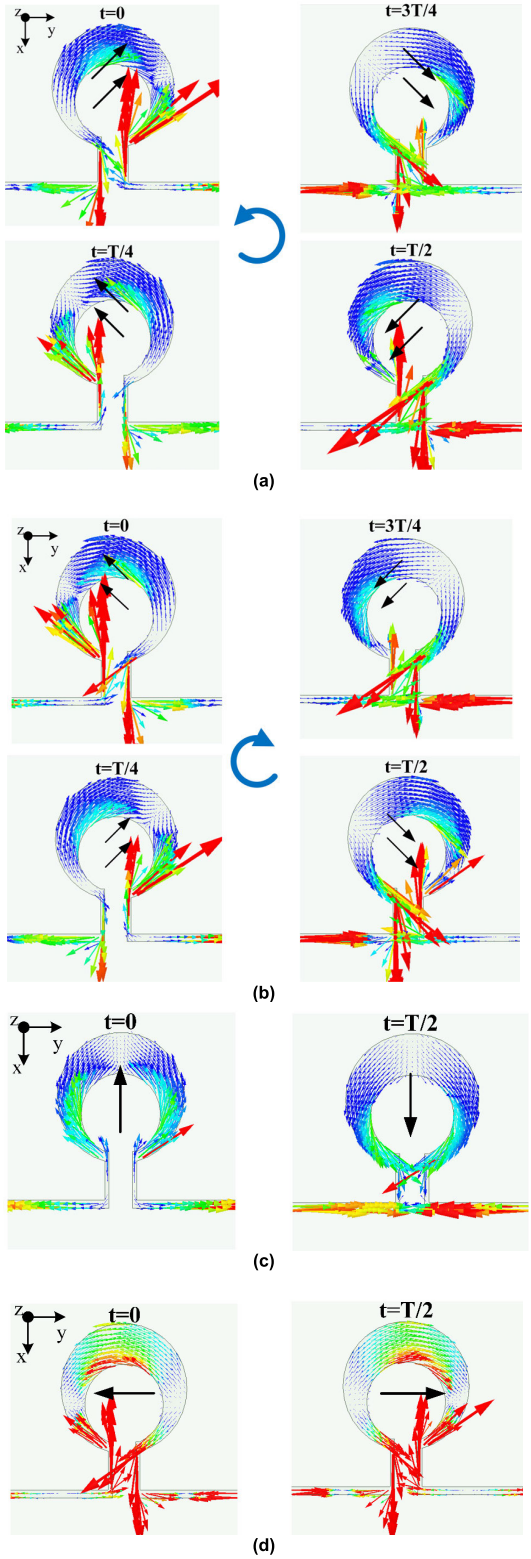

FIGURE 2. The instantaneous current distribution of unit cell fed by different polarization. (a) Port 2 fed (RHCP). (b) Port 1 fed (LHCP). (c) Two ports are fed in same phase (X-LP). (d) Two ports are fed out of phase (Y-LP).

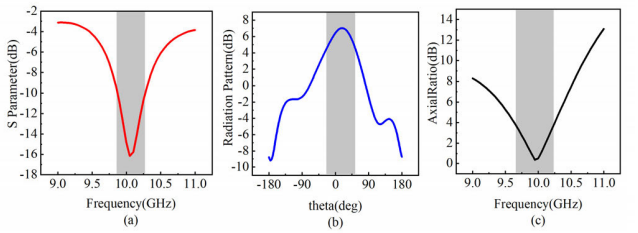

FIGURE 3. (a) The reflection coefficient, (b) radiation pattern and (c) axial ratio plots of unit cell.

main direction of the instantaneous current distributions at this moment.

As shown in Figure 2 (a), in order to fields rotate counterclockwise generate to RHCP [17], the port 1 is matched terminated and port 2 is fed. Next, the unit cell can rotate clockwise to generate LHCP when port 1 is fed and port 2 is matched terminated, as shown in Figure 2(b). In Figure 2(c), when two ports are fed in the same phase, the X-Linear polarization(X-LP) will be excited. Then, when two ports are fed out-of-phase, Y-Linear polarization (Y-LP) will be appeared, which is shown in Figure 2 (d). Thus, if the unit cell is properly arranged, a polarization switchable antenna array can be formed.

When realizing the X-LP and Y-LP of the unit cell, the two ports of the antenna should be fed at the same time. Two ports are fed in same phase of X-LP. Two ports are fed out of phase of Y-LP. It is necessary to connect power divider and phase shifter. The power divider can feed two ports of the circular array at the same time. The phase shifter can realize different feed phases.

The simulated reflection coefficient, gain, radiation pattern and axial ratio plots of unit cell are shown in the Figure 3. The reflection coefficient of the unit cell is −16dB. The 10 dB impedance bandwidth (BW) and 3 dB axial ratio bandwidth (ARBW) of the unit cell are 4% and 5%. The peak gain is 7dB. The 3dB beam width is 87deg.

III. CIRCULAR ARRAY GEOMETRY

A. CIRCULAR ARRAY

The proposed unit-cell structure has the feature of polarization switchable by adjusting the feed. The multi-polarization antenna can be designed thought these cells. In Figure.4, the antenna structure is demonstrated by designing and building an array of seven patch elements, two-port microstrip feed, and a ground plane. The structure was simulated by full-wave software HFSS2018 verify numerical results. The angle between adjacent elements is 45°. The elements are connected by microstrip lines. The antenna is design on 1.5-mm-thick F4B substrate ($\varepsilon r = 2.65$, $\tan\delta = 0.0015$).

In Figure 5(a), a prototype of the antenna is fabricated. The simulated absolute current strength colormap for array is shown in Figure 5(b).

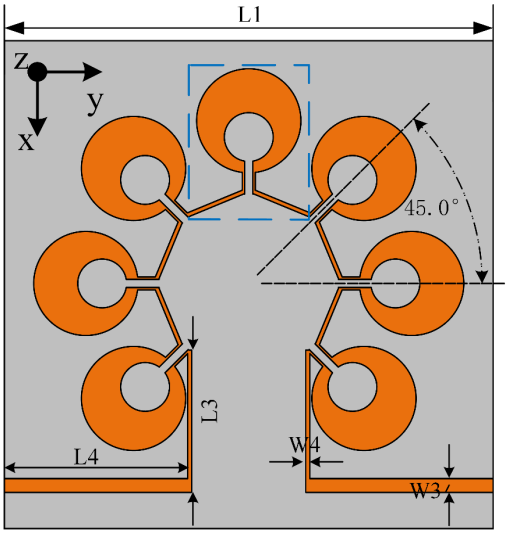

FIGURE 4. Circular array overall configuration. The antenna design parameters are: W3 = 1.7mm, W4 = 0.5 mm, L1 = 60mm, L3 = 17.5mm, L4 = 23.0mm.

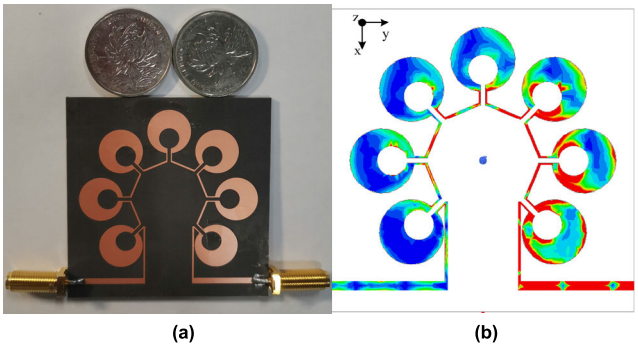

FIGURE 5. (a) The photo of antenna material object. (b) Simulated absolute current strength colormap for a patch element (the surface current intensity of the part shown in red is high).

The power radiated by each element P can be expressed as follows

$$P \propto \frac{1 - (|S_{11}|^2 + |S_{21}|^2)}{1 - |S_{11}|^2} \tag{1}$$

When $|S_{11}|$ is small enough, the equation can be simplified as

$$P \propto 1 - |S_{21}|^2 \tag{2}$$

The values of $|S_{21}|$ will relate the power radiated by elements. The power radiated by elements will be large when values of $|S_{21}|$ is small enough. The $|S_{21}|$ of antenna is expected to decrease as the line length increases. Considering the size of the unit-cell, the layout of the circular array with Ref. [13], it was finally decided to select seven unit-cell. The circular array structure is demonstrated by designing and building an array of seven patch elements, two-port microstrip feed, and a ground plane. The angle between adjacent elements is 45°. The elements are connected by microstrip lines.

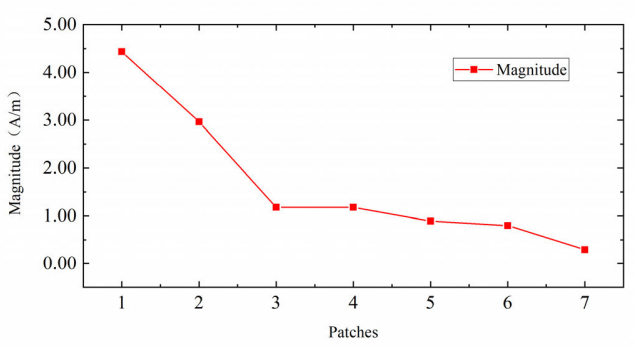

FIGURE 6. The simulated magnitude of the surface current density on the same points to each unit cell.

At this time, one port excites power to the other port. The energy of the antenna will be radiated out through seven-unit structures. As shown in Figure 6, the simulated surface current density magnitude at the same point of each patch decreases gradually, which can verify this viewpoint.

The patch array is built by eccentric rings which can realize the performance of circular polarization. The dual-port feeding allows us to switch the polarization of the antenna. When the seven unit-cell are connected end to end, the polarization property of the unit-cell is not damaged. By adjusting the feed, the circular polarization and linear polarization of the circular array can still be switched. The polarization property of circular array is the same as that of unit cell.

The reflection coefficient, axial ratio and radiation pattern of unit cell and circular array are shown in the table 1. Compared with the unit-cell, the BW and ARBW of the circular array are significantly widened. The reflection coefficients of the two antennas are basically the same. The peak gain of the circular array is much higher than that of the unit-cell, and the radiation energy is more concentrated.

B. 4 × 4 MIMO

In part A, a circular array composed of seven patch elements and two-port microstrip feed is proposed. Then, the 4 × 4 MIMO circular array which is composed of four circular arrays is proposed. And it has 8 feed ports in total. As shown in Figure 7, the distance between the array elements is D. When designing the array antenna, the distance between the array elements should follow certain rules. First, the element radiation of array does not affect each other. Second, there is no grid lobe in the antenna pattern. Third, the size of the array antenna is small and the structure is compact.

A parametric study on the circular array separation D for the axial ratio is carried out for the 4 × 4 MIMO array. In Figure 8, the effect of varying D on the axial ratio is shown. Considering the axial ratio bandwidth and antenna radiation pattern, D =52mm is selected. The reflection coefficient

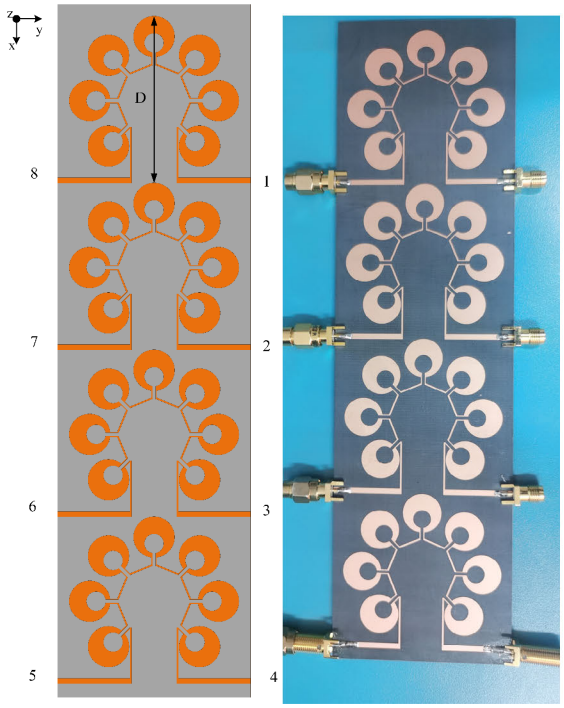

FIGURE 7. (a) 4 × 4 MIMO array separated by D = 52 mm. (b) The photo of 4 × 4 MIMO.

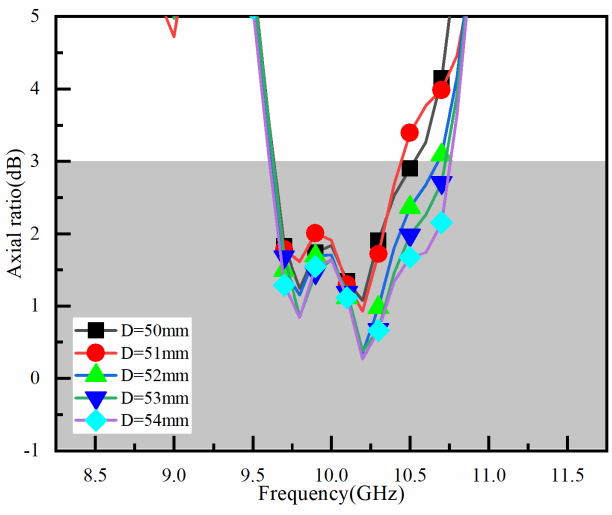

FIGURE 8. Effect of different separation D on the axial ratio of the 4 × 1 circular array.

$|S_{11}| < -10$ dB and interport isolation $|S_{n+1,n}| < -23$ dB ($1 \leq n \leq 3$) is obtained with D = 52 mm throughout the desired bandwidth of simulated results.

As shown in Figure 7, the 4 × 4 MIMO array has 8 feed ports, which are independent of each other. The principle of polarization switching of 4 × 4 MIMO array antenna is same with rule of circular array antenna. When ports 1, 2, 3 and 4 are fed normally, each circular array will form right circular polarization, resulting in a right circular polarization of the 4 × 4 MIMO array. Similarly, when the ports 4, 5,

TABLE 1. Performance comparisons between unit cell and circular array.

Antenna	BW	Reflection Coefficient(dB)	ARBW	Peak Gain(dB)	Isolation (dB)	3 dB beam width(°)
Unit-cell	4%	-16dB	5%	7.0	-3.7	87
Circular array	13%	-14dB	13%	11.5	-32.6	32

6 and 7 are fed normally, the 4 × 4 MIMO array antenna will form left-handed circular polarization. When all ports are fed at the same phase, the 4 × 4 MIMO array shows X-LP. When all ports are fed at the same time, the feeding phase of one side port of the array antenna is opposite to that of the other side port. The 4 × 4 MIMO array will form Y-LP. The above is the polarization switching regular of the 4 × 4 MIMO array.

In order to observe the performance characterization of the 4 × 4 MIMO array, envelop correlation coefficient (ECC) is an important parameter, which should be minimized as much as possible.

The ECC for the MIMO array is calculated using the formula given in Equation (3). Figure 9 depicts the simulated ECC plots obtained from S-parameters. It can be seen that the ECC is less than 0.0002 for the entire radiating bands, the range from 9.4 to 10.7 GHz. The obtained low value of the envelop correlation coefficient leads to strong diversity for 4 × 4 MIMO array.

$$\mathrm{ECC} = \frac{\left|S_{\mathrm{ii}}^{*}S_{ij} + S_{ji}^{*}S_{jj}\right|}{(1-(|S_{ii}|^2 + \left|S_{ji}\right|^2))(1-(\left|S_{jj}\right|^2 + \left|S_{ij}\right|^2))} \tag{3}$$

Then, the channel capacity loss (CCL) is another important parameter. CCL is the upper threshold of data rate at which signal can be constantly transmitted without incurring significant error. The CCL can be defined by Equation (4).

$$CCL = -\log_2 \left|\psi^R\right| \tag{4}$$

where ψ^R is the receiving antenna correlation matrix, which is shown in Equation (5)

$$\psi^R = \begin{bmatrix} a_{ii} & a_{ij} \\ a_{ji} & a_{jj} \end{bmatrix} \tag{5}$$

where $a_{ii} = (1 - |S_{ii}|^2 - \left|S_{ij}\right|^2)$ and $a_{ij} = -(S_{ii}^{*}S_{ij} + S_{ji}^{*}S_{ij})$.

Figure 9(b) shows the simulated CCL of 4 × 4MIMO array. It can be seen that the value of CCL is less than 0.2b/s/Hz for the 4 × 4 MIMO array. The obtained CCL can make the antenna suitable for MIMO applications.

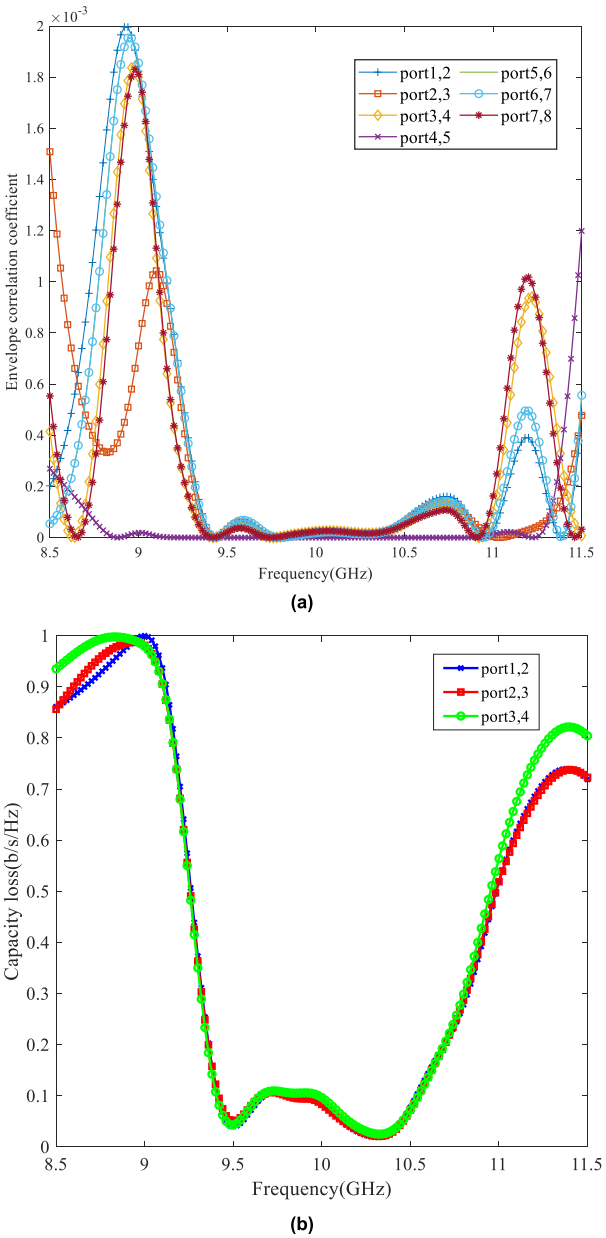

FIGURE 9. The results of 4 × 4 MIMO (a) ECC; (b) CCL.

IV. EXPERIMENTAL RESULTS

The S parameters, antenna pattern, axial ratio and gain of the antenna are obtained through measured in a far-field anechoic chamber. Prepare two speakers with the same frequency range of 8-12GHz to measure the axial ratio, gain and radiation pattern of the array. The axis ratio and gain of the antenna array are measured at 20 frequency points, one for each 0.1GHz (9.0-11.0GHz). The circular polarization and linear polarization radiation patterns of circular array and 4 × 4

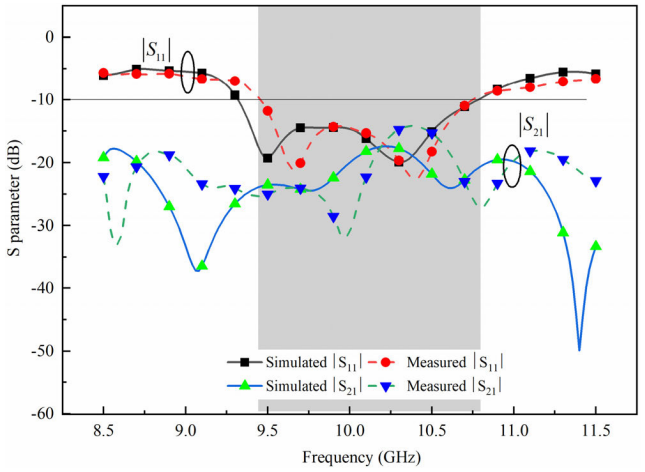

FIGURE 10. The simulated and measured S-parameters of the array.

MIMO array are measured at the central frequency of 10GHz. During the circular array measured, it is necessary to connect power divider and phase shifter between SMA connector and vector network analyzer. The power divider can feed 8 ports of the circular array at the same time. The phase shifter can realize different feed phases. The details are as follows.

A. S-PARAMETERS

The antenna has been fabricated and measured characterized to confirm the design. The measured and simulated S-parameters of this circular array are shown in Figure 10. The FBW of circular array is 13%. The array measured reflection coefficients $|S_{11}|$ are lower than −10 dB and the transmission coefficients $|S_{21}|$ are lower than −15 dB from 9.4 to 10.7 GHz, which explains that the antenna has high port isolation performance for dual CP operation. The measured results have little different between simulated results because the extra losses are caused by the inhomogeneity of the rough metal layer. What is more important, the measured results and simulated ones for the antenna show good agreement.

Then the simulated and measured S-parameters of 4 × 4 MIMO array are presented in Figure 11, respectively. The S-parameters include the impedance matching and interport isolation between the adjacent array elements. From 9.4 to 10.7 GHz, the reflection coefficients $|S_{nn}|$ are smaller than −10 dB and interport isolation $|S_{n+1,\,n}|$ are better than −20 dB for the simulated and measured results.

B. RADIATION PATTERNS

In Figure 12, the measured and simulated radiation patterns in the $\varphi = 0$deg and $\varphi = 90$deg for RHCP, LHCP, X-LP and Y-LP at 10 GHz are shown. The measured 3 dB beamwidth is about 32° and 29° in the $\varphi =$ 0deg and $\varphi =$ 90deg of CP, respectively. The sidelobe level in the pattern is mostly lower than −10dB. The D-value between the co-

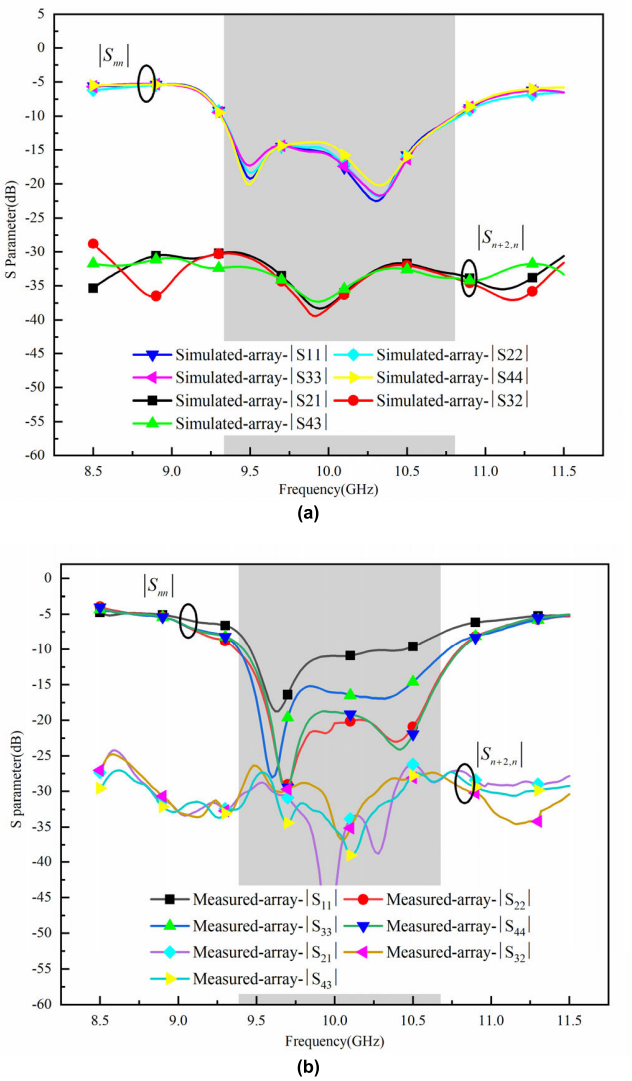

FIGURE 11. (a) Simulated and (b) Measured S-parameters for different branches of the 4 × 1 array antenna.

polarized component and the cross-polarization component is about 15dB. The simulated and measured results are in good agreement.

The LP measured 3 dB beamwidth is about 25° and 36° in the $\varphi =$0deg and $\varphi = 90$deg. The co-polarized component is approximately 12 dB higher than the cross polarized one. The measured results have little different between simulated results because a power divider and some lossy transmission lines are used to feed electricity during the measure process. Increasing the D-value between co-polarized component and cross polarization is also one of the priorities of future work.

The 4 × 4 MIMO array radiation patterns are shown in Figure 13. The measured results meet the simulated requirements. The simulated 3 dB gain-beamwidth in the $\varphi =$ 0deg is 7.8°, 8°, 8.1°, and 7.6° and the 3 dB gain-beamwidth in the $\varphi = 90$deg is 30.6°, 30.7°, 21.4°, and 21.9° for the RHCP, LHCP, X-LP, and Y-LP polarization, respectively.

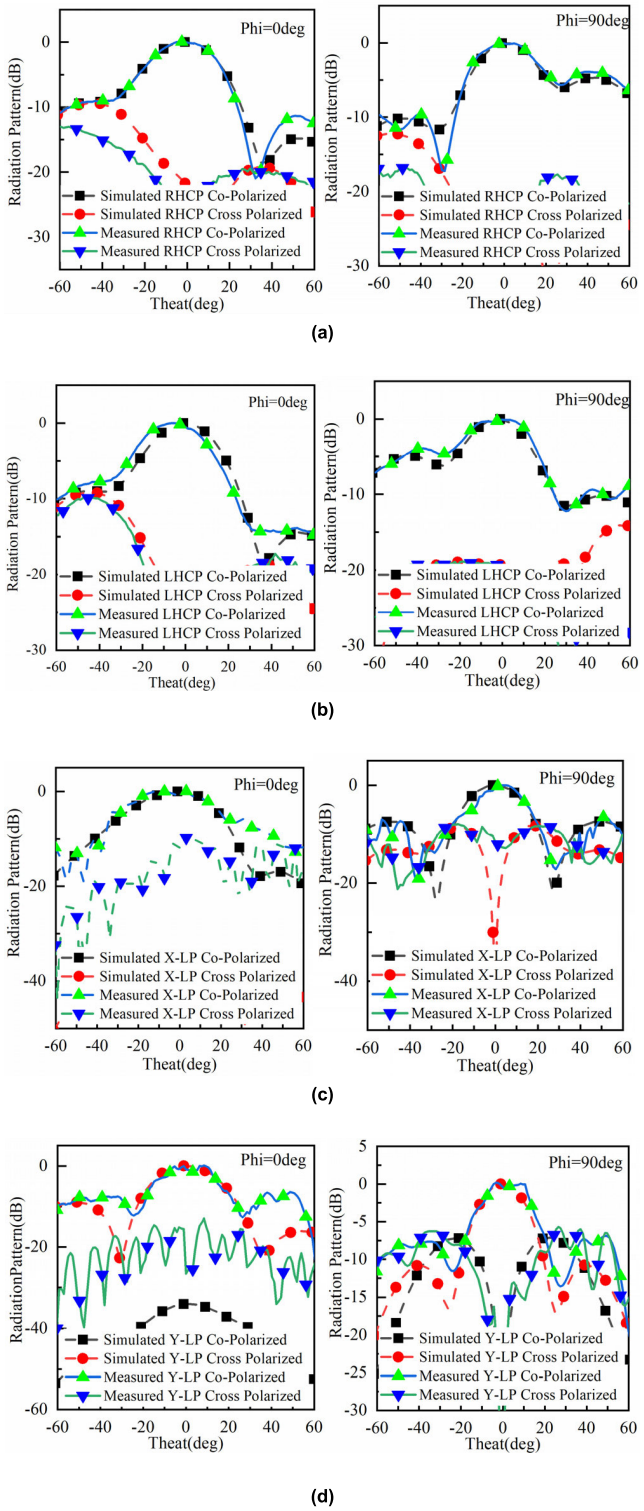

FIGURE 12. The simulated and measured normalized radiation patterns in the $\varphi = 0$ deg and $\varphi = 90$ deg of circular array at 10GHz (a) RHCP. (b) LHCP. (c) X-LP. (d) Y-LP.

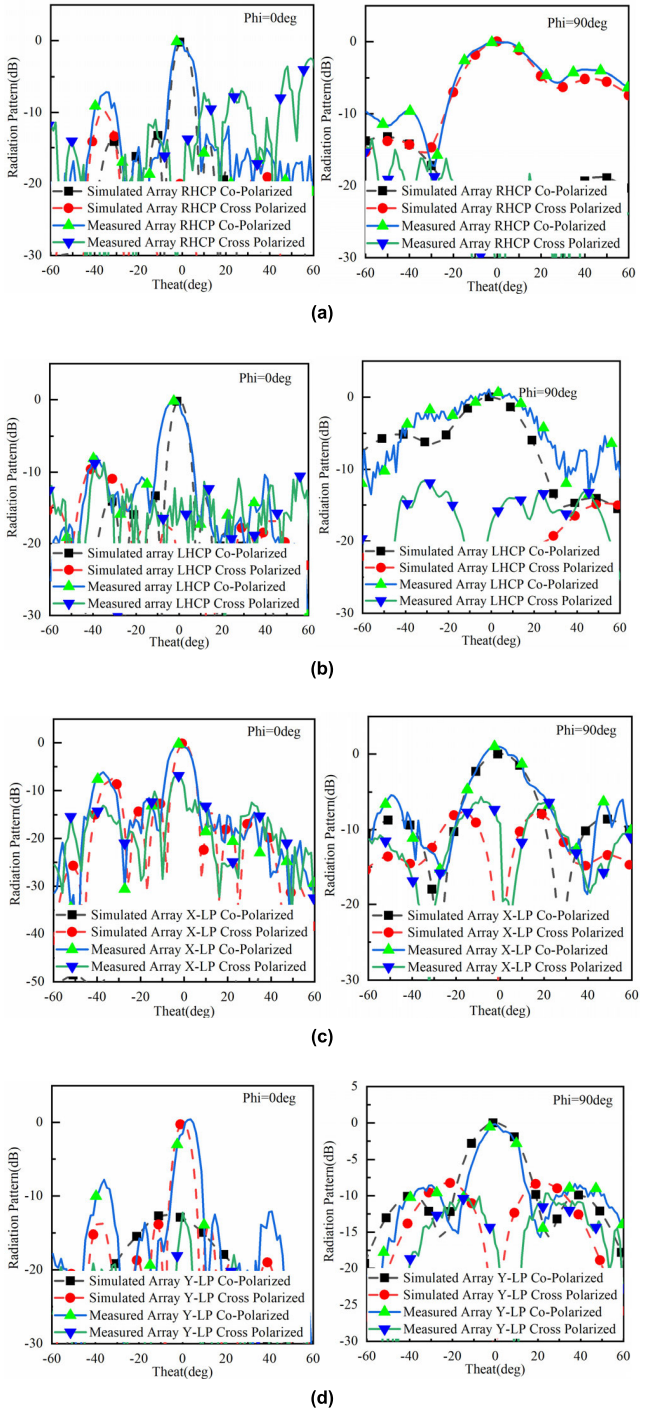

FIGURE 13. Simulated and measured 10-GHz normalized radiation patterns in the xz- and yz-planes of 4 × 4 MIMO array antenna (a) RHCP. (b) LHCP. (c) X-LP. (d) Y-LP.

Then, the measured 3 dB gain-beamwidth in the $\varphi = 0$deg is 7.2°, 8.8°, 9.2°, and 8.4° and the 3 dB gain-beamwidth in the $\varphi = 90$deg is 30.7°, 31.8°, 21.9°, and 20.6° for the RHCP, LHCP, X-LP, and Y-LP polarization, respectively. The sidelobe level is less than −10dB. The co-polarized component is approximately 15 dB higher than the cross polarized one. The simulated and measured results are in good agreement.

During the circular array measured, the power divider can feed 8 ports of the 4 × 4 MIMO array at the same time. The

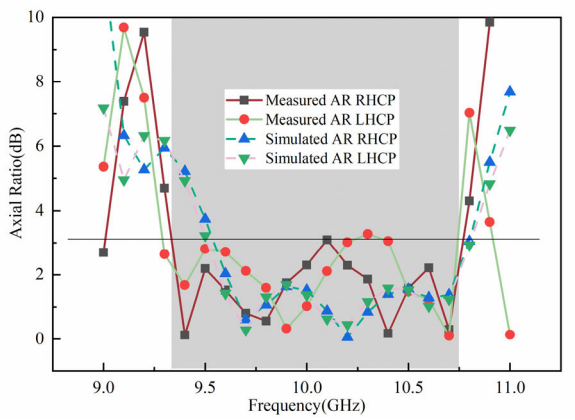

FIGURE 14. Simulated and measured AR.

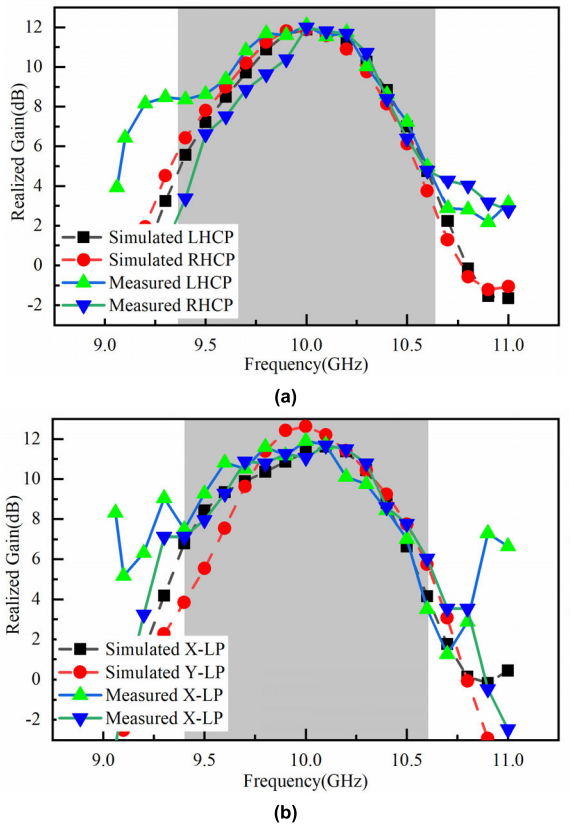

FIGURE 15. Simulated and measured realized gain for different polarizations.

phase shifter can realize different feed phases. Finally, the data are calculated, processed and plotted.

C. AXIAL AND GAIN

Generally, the measured of the axial ratio (AR) is used to detect the circular polarization characteristic. Simulated and measured axial ratio in mentioned bands are presented in Figure 14 of circular array. The 3-dB AR bandwidth ranges from 9.4 to 10.7 GHz (13%), respectively. The axial ratio of

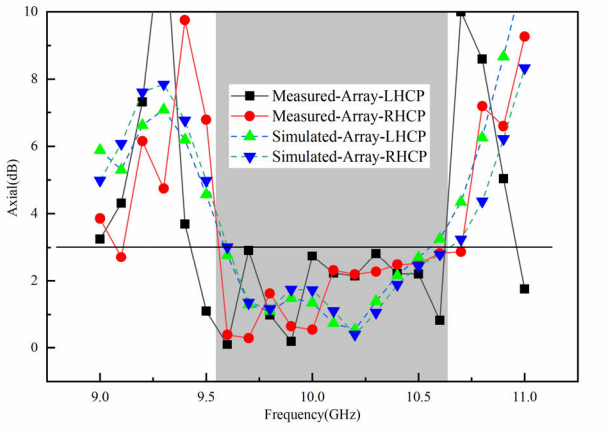

FIGURE 16. Simulated and measured AR.

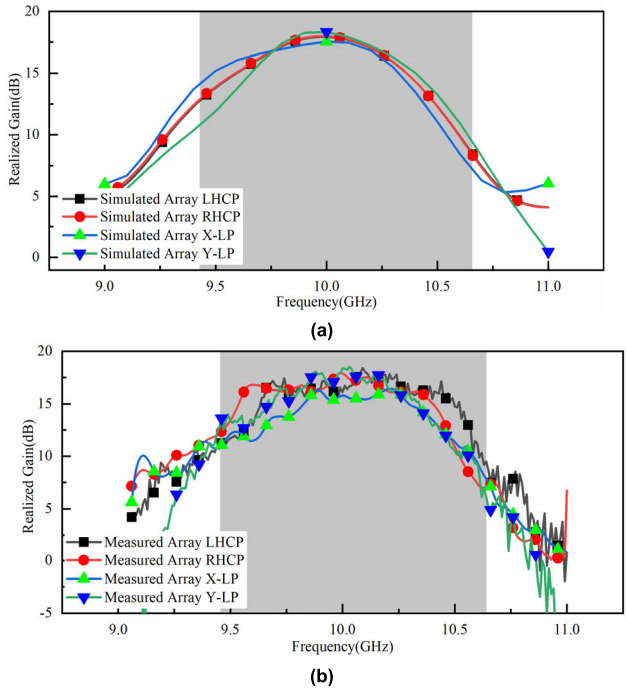

FIGURE 17. (a) and (b) simulated and measured realized gain for different polarizations of 4 × 1 array antenna.

proposed antenna meets the requirements of most circularly polarization communication systems.

The simulated and measured realized gain broadside of RHCP, LHCP are shown in Figure 15(a), and the X-LP, Y-LP are shown in Figure 15(b). The measured CP realized gain is about11.5 dB at 10GHz, and the LP realized gain is about 11dB at 10GHz. The gain within the bandwidth is larger than 6dB.

The measured and simulated axial ratio (AR) and realized gain at bands of 4 × 4 MIMO array antenna are shown in Figure 16. The 3-dB AR bandwidth ranges from 9.6 to 10.6 GHz (10%), respectively. The simulated and measured broadside RHCP, LHCP, X-LP, and Y-LP Linear-X realized gain is plotted in Figure 17(a) and (b). The measured realized gain is maintained between 12.5 and 17.5 dB within the

TABLE 2. Comparisons with some previous antennas.

Ref	BW	ARBW	Peak Gain(dB)	Isolation (dB)	Polarization Switchable	Dimension ($\lambda_0 * \lambda_0$)
[3]	24%	16%	9.6	-7	no	1.45*1.45
[5]	27.9%	/	5.2	-32.6	yes	1.6*1.3
[6]	7.95%	0.72%	5.7	/	no	0.44*0.48
[10]	14.7%	14.7%	10.7	-12	yes	5.9*2.8
[13]	6.57%	6.7%	11.8	-20	no	3.5*2.8
Circular array	13%	13%	11.5	-15	yes	3.1*3.1

operational bandwidth. The simulation results of the gain are in good agreement with the measurement results.

In section II, a unit-cell is proposed which gain is about 6dB. Then we use the unit-cell to build a circular array. The gain of circular array is about 11dB. Finally, we use the circular array to design a 4 × 4 MIMO array. The gain of 4 × 4 MIMO array is about 16dB.

The table 2 is obtained by summarizing and comparing the existing antenna work. Obviously, the proposed antenna has some advantages, such as wide frequency bandwidth and AR bandwidth. The polarization of proposed antenna can be switched. And it has lager isolation.

V. CONCLUSION

This paper proposed a multi-polarization switchable and traveling-wave series-fed antenna. Firstly, an eccentric ring unit cell structure which can realize polarization switchable is proposed. By suitable excitation of the ports, the multi-polarization switchable performance can be realized. Then, the unit structure is arranged in circular array. This antenna can realize the polarization switchable without switch controlling. The transmission coefficient is lower than −14 dB in the mentioned frequencies. The axial ratios are lower than 3dB measured. Next, the 4 × 4 MIMO array can be built by circular array to increase gain and focus energy. In the future, the research focus of antenna work will be to increase the D-value between co-polarized component and cross polarization. Multiploidization switched antenna is more suitable for complex communication environment, such as ship satellite, radar and civilian vehicle speed monitoring. The antenna has the function of polarization switching, which can send or receive signals of arbitrary polarization for information matching.

ACKNOWLEDGMENT

The authors would like to thank teachers and classmates for their help during the fabrication and measurement process.

REFERENCES

[1] J.-D. Zhang, W. Wu, and D.-G. Fang, "Dual-band and dual-circularly polarized shared-aperture array antennas with single-layer substrate," *IEEE Trans. Antennas Propag.*, vol. 64, no. 1, pp. 109–116, Jan. 2016.

[2] Q. Liu, J. Shen, J. Yin, H. Liu, and Y. Liu, "Compact 0.92/2.45-GHz dual-band directional circularly polarized microstrip antenna for handheld RFID reader applications," *IEEE Trans. Antennas Propag.*, vol. 63, no. 9, pp. 3849–3856, Sep. 2015.

[3] C. Zhang, X. Liang, X. Bai, J. Geng, and R. Jin, "A broadband dual circularly polarized patch antenna with wide beamwidth," *IEEE Antennas Wireless Propag. Lett.*, vol. 13, pp. 1457–1460, 2014.

[4] M. Midya, G. Sen, M. Gangopadhyaya, and M. Mitra, "A circularly polarized wide slot antenna for WLAN applications," in *Proc. 5th Int. Conf. Electron., Mater. Eng. Nano-Technol. (IEMENTech)*, Sep. 2021, pp. 1–3.

[5] Y. Li, Z. Zhang, W. Chen, Z. Feng, and M. F. Iskander, "A dual-polarization slot antenna using a compact CPW feeding structure," *IEEE Antennas Wireless Propag. Lett.*, vol. 9, pp. 191–194, 2010.

[6] Z. Zhao, F. Liu, J. Ren, Y. Liu, and Y. Yin, "Dual-sense circularly polarized antenna with a dual-coupled line," *IEEE Antennas Wireless Propag. Lett.*, vol. 19, no. 8, pp. 1415–1419, Aug. 2020.

[7] Z.-X. Liang, D.-C. Yang, X.-C. Wei, and E.-P. Li, "Dual-band dual circularly polarized microstrip antenna with two eccentric rings and an arc-shaped conducting strip," *IEEE Antennas Wireless Propag. Lett.*, vol. 15, pp. 834–837, 2016.

[8] H. Yang, Y. Fan, and X. Liu, "A compact dual-band stacked patch antenna with dual circular polarizations for BeiDou navigation satellite systems," *IEEE Antennas Wireless Propag. Lett.*, vol. 18, no. 7, pp. 1472–1476, Jul. 2019.

[9] J.-F. Li, D.-L. Wu, G. Zhang, Y.-J. Wu, and C.-X. Mao, "A left/right-handed dual circularly-polarized antenna with duplexing and filtering performance," *IEEE Access*, vol. 7, pp. 35431–35437, 2019.

[10] Y. Shen, S.-G. Zhou, G.-L. Huang, and T.-H. Chio, "A compact dual circularly polarized microstrip patch array with interlaced sequentially rotated feed," *IEEE Trans. Antennas Propag.*, vol. 64, no. 11, pp. 4933–4936, Nov. 2016.

[11] P. Hallbjorner, I. Skarin, K. From, and A. Rydberg, "Circularly polarized traveling-wave array antenna with novel microstrip patch element," *IEEE Antennas Wireless Propag. Lett.*, vol. 6, pp. 572–574, 2007.

[12] R. T. Cameron, T. A. Sutinjo, and M. Okoniewski, "A circularly polarized broadside radiating 'herringbone' array design with leaky-wave approach," *IEEE Antennas Wireless Propag. Lett.*, vol. 9, pp. 826–829, 2010.

[13] Y.-H. Yang, B.-H. Sun, and J.-L. Guo, "A low-cost, single-layer, dual circularly polarized antenna for millimeter-wave applications," *IEEE Antennas Wireless Propag. Lett.*, vol. 18, no. 4, pp. 651–655, Apr. 2019.

[14] T. Yuan, N. Yuan, and L.-W. Li, "A novel series-fed taper antenna array design," *IEEE Antennas Wireless Propag. Lett.*, vol. 7, pp. 362–365, 2008.

[15] Y.-H. Yang, J.-L. Guo, B.-H. Sun, Y.-M. Cai, and G.-N. Zhou, "The design of dual circularly polarized series-fed arrays," *IEEE Trans. Antennas Propag.*, vol. 67, no. 1, pp. 574–579, Jan. 2019.

[16] G. Mishra, S. K. Sharma, and J.-C.-S. Chieh, "A high gain series-fed circularly polarized traveling-wave antenna at W-band using a new butterfly radiating element," *IEEE Trans. Antennas Propag.*, vol. 68, no. 12, pp. 7947–7957, Dec. 2020.

[17] G. Mishra and S. K. Sharma, "A multifunctional full-polarization reconfigurable 28 GHz staggered butterfly 1-D-beam steering antenna," *IEEE Trans. Antennas Propag.*, vol. 69, no. 10, pp. 6468–6479, Oct. 2021.

XIN GUAN received the B.S. degree in information warfare technology from Shenyang Ligong University, Shenyang, in 2018, and the master's degree from Northeastern University, Qinhuangdao, in 2021. She is currently pursuing the Ph.D. degree with the Beijing Institute of Technology, Beijing, China. She studied the content of theory of antenna array and polarization. Her research interests include antenna array, circular polarization, and endfire antenna.

ZHENGHUI XUE received the B.S. and Ph.D. degrees from the School of Information and Electronics, Beijing Institute of Technology. He is currently a Professor, a Doctoral Supervisor, and the discipline Leader of the School of Integrated Circuits and Electronics, Institute of Electronic Science and Technology, Beijing Institute of Technology. His research interests include theory of electromagnetic field, microwave device design, and research of antenna array.

WU REN received the B.S. and Ph.D. degrees in electromagnetic field and microwave technology from the Beijing Institute of Technology, Beijing, China, in 1998 and 2003, respectively. He is currently an Associate Professor with the School of Integrated Circuits and Electronics, Beijing Institute of Technology. His current research interests include computational electromagnetics, microwave and millimeter-wave techniques, electromagnetic compatibility, and metamaterials.

WEIMING LI received the B.S. degree in mathematical from Jiangxi Normal University, Nanchang, China, in 1988, and the Ph.D. degree in electromagnetic field and microwave technology from the Beijing Institute of Technology, Beijing, China, in 2001. He is currently an Associate Professor with the Electronic Engineering Department, Beijing Institute of Technology. He has authored or coauthored over 30 articles. His current research interests include computational electromagnetics and wideband antenna techniques.